Single photon radioluminescence

II. Signal detection and biological applications

Zahra Shahrokh, S. Bicknese, Stephen B. Shohet, and A. S. Verkman

Departments of Laboratory Medicine, Medicine, and Physiology, and the Cardiovascular Research Institute, University of California, San Francisco, California USA

ABSTRACT A quantitative theory for excitation of fluorescent molecules by beta decay electrons is reported in the accompanying manuscript; experimental detection methods and biological applications are reported here. The single photon signals produced by an excited fluorophore (single photon radioluminescence, SPR) provide quantitative information about the distance between radioisotope and fluorophore. Instrumentation was constructed for SPR signal detection. Photons produced in a 0.5-ml sample volume were detected by a cooled photomultiplier and photon counting electronics. To minimize electronic noise and drift for detection of very small SPR signals, a mechanical light chopper was used for gated-signal detection, and a pulse height analyzer for noise rejection. SPR signals of ~1 cps were reproducibly measurable. The influence of inner filter effect, sample turbidity, and fluorophore environment (lipid, protein, and carbohydrate) on SPR signals were evaluated experimentally. SPR was then applied to measure lipid exchange kinetics, ligand binding, and membrane transport, and to determine an intermolecular distance in an intact membrane. (*a*. Lipid exchange kinetics.) Transfer of 12-anthroyloxystearic acid (12-AS) from sonicated lipid vesicles and micelles to vesicles containing ^{3}H-cholesterol was measured from the time course of increasing SPR signal. At 22°C, the half-times for 12-AS transfer from vesicles and micelles were 3.3 and 1.1 min, respectively. (*b*. Ligand binding.) Binding of ^{3}H-oleic acid to albumin in solution, and ^{3}H-2,2′-dihydro-4,4′-diisothiocyanodisulfonic stilbene (^{3}H-H$_2$DIDS) to band 3 on the erythrocyte membranes were detected by the radioluminescence of the intrinsic tryptophans. The SPR signal from 5 μCi ^{3}H-oleic acid bound to 0.3 mM albumin decreased from 13 ± 2 cps to 3 ± 2 cps upon addition of nonradioactive oleic acid, giving 2.7 high affinity oleic acid binding sites per albumin. The SPR signal from 1 μCi ^{3}H-H$_2$DIDS bound selectively to erythrocyte band 3 in erythrocyte ghosts (1.5 mg protein/ml) was 2.2 ± 0.8 cps. (*c*. Membrane transport.) Dilution of J774 macrophages loaded with ^{3}H-3-O-methylglucose and BCECF gave a decreasing SPR signal with a half-time of 81 s due to methylglucose efflux; the SPR measurement of the efflux rate was in agreement with a conventional tracer efflux rate determination by filtration. 20 μM cytochalasin B inhibited efflux by 97%. (*d*. Distance determination.) The SPR signal from erythrocyte membranes labeled with 27 μCi ^{3}H-oleic acid and 10 μM of fluorescein-labeled wheat germ agglutinin was 5.7 ± 0.5 cps, giving an average glycocalyx-to-bilayer distance of 5 nm. The results establish methods for experimental detection of SPR signals and demonstrate the applications of radioluminescence to the measurement of lipid exchange kinetics, ligand binding, membrane transport, and submicroscopic distances in intact membranes in real time.

INTRODUCTION

As demonstrated in the previous paper, there is a finite probability for excitation of a fluorophore located in the path of an electron produced by beta decay. The decay of tritium produces electrons with a continuous distribution of energies up to 18.5 keV. When these low energy electrons move through an aqueous environment, the effective maximum distance over which excitation of a reporter fluorophore can occur is 1–2 μm; for distances < 1 μm, the probability of fluorophore excitation is nearly proportional to the inverse square of the distance between the donor tritium radioisotope and the acceptor fluorophore. The probability of fluorescence excitation also depends upon the nature of the reporter fluorophore and its physical environment.

The intrinsic distance information contained in measurements of single photon radioluminescence (SPR) can be exploited to develop a number of novel biological applications. Von Tscharner and Radda (1980, 1981) examined the physical state of phospholipids in the condensed phase of micelles and small lipid vesicles by incorporating tritiated phospholipids and lipophilic fluorophores (anthroyloxy fatty acids) in the lipid mixture. Because of the close proximity between tritium donors and fluorescent acceptors in the micelle system, SPR signals were relatively large, with ~10^3 recorded counts per second (cps). SPR signals are considerably smaller in the new applications proposed here.

The measurement of SPR should provide a molecular ruler for distance determination in biological systems. As modeled in the previous paper, donor-acceptor distances greater than 100 nm should be measurable, greatly extending the maximum distance of ~10 nm measurable by fluorescence resonance energy transfer (Stryer, 1978). The ability to measure large distances is particularly useful in studies of membrane-cytoskeletal interactions and protein-protein distances in intact membranes which often exceed 10 nm. Because the production of an SPR signal requires proximity between the donor radioisotope and the acceptor fluorophore, it should be possible to detect ligand-receptor binding, or the formation of other molecular complexes, in intact systems and in real time. Similarly, SPR should provide a simple approach to study the transport of molecules across cell membranes; for example, the influx of a tritiated solute into a fluorescently labeled cell should produce a time-dependent increase in SPR signal. Other po-

Address correspondence to Zahra Shahrokh, Ph.D., MacMillan-Cargill Hematology Research Laboratory, 1217 Health Sciences East Tower, University of California, San Francisco, CA 94143-0134.

tential applications of SPR include measurement of the kinetics of lipid exchange between vesicles and cells, and the rates of vesicle fusion.

The detection of SPR signals is made difficult by the small number of single photon events in many biological samples and the multiple sources of background signal. Similar concerns apply to the measurement of single photon events in high energy physics and astrophysics. The SPR detection apparatus reported here consists of a high sensitivity, low noise photomultiplier and photon counting electronics. In addition, to optimize the detection of small SPR signals which may require long acquisition times, the instrument incorporates gated-signal detection by a mechanical light chopper and signal discrimination by multi-channel analysis.

This paper reports: (*a*) the construction and performance of an SPR detection apparatus; (*b*) the evaluation of special concerns in the application of SPR to biological samples, including sample turbidity, absorbance and environment effects; and (c) biological applications of SPR including lipid exchange kinetics, ligand binding, solute transport across cell membranes, and quantitative distance determination. The results demonstrate the utility of single photon radioluminescence measurements in biological samples.

MATERIALS

^{3}H-D-glucose (15 Ci/mmol), ^{3}H-oleic acid (10 Ci/mmol), and ^{14}C-urea (55 mCi/mmol) were purchased from Amersham Corp. (Arlington Heights, IL), ^{3}H-*O*-methyl-D-glucose (79 Ci/mmol) and ^3H_2O (1 Ci/g) were from New England Nuclear (Boston, MA), and ^{3}H-H_2DIDS (2 Ci/mmol) was from Research & Development Limited Partnership (Toronto, Canada). The anthroyloxy stearic and palmitic fatty acids, BCECF-AM, fluorescein, fluorescein-labeled dextran and wheat germ agglutinin were purchased from Molecular Probes Inc. (Eugene, OR). Phospholipids were obtained from Avanti Polar Lipids (Alabaster, AL). All other chemicals and reagents were purchased from Sigma Chemical Co. (St. Louis, IL). Samples for radioluminescence measurements were contained in cylindrical glass vials (0.7 ml capacity, 6.8 mm inner diameter, 30 mm height, Kimble No. 60831D) with plastic snap caps.

EXPERIMENTAL METHODS

Instrumentation

The SPR signal detection system is shown schematically in Fig. 1. The glass sample container was positioned at a distance of 13.5 mm from the quartz window of a thermoelectric cooled photomultiplier housing (temperature −20°C, model Fact-50; Thorn-EMI, Rockaway, NJ) containing a 13-dynode end-on photomultiplier (9235QA, active surface area 15.9 cm^2, dark current 3 nA at −20°C, gain 10^7; Thorn-EMI). Photomultiplier voltage was maintained at 1,100 V by a model 126 Pacific Instruments H.V. power supply (Concord, CA). To maximize collected light, a 71-mm diameter concave spherical, front-surfaced mirror with a 30-mm focal length (Melles-Griot, Irvine, CA) was positioned 14 mm behind the sample. A mechanical light chopper (model 9479; EG & G, Oakridge, TN) with a half-closed blackened aluminum blade was placed between the sample and the photomultiplier for signal gating. The light chopper provided a +5 V gating pulse for detector timing.

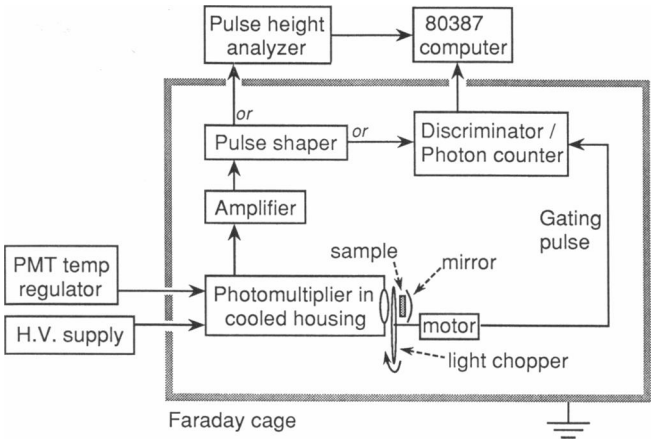

FIGURE 1 Schematic of instrumentation for detection of single photon radioluminescence signals. The sample is placed between the front window of a cooled photomultiplier housing and a concave mirror. A gated signal is produced by a mechanical light chopper placed between the sample and the photomultiplier. The signal is amplified and processed by discriminator/photon counter or pulse height analyzer. See text for details.

The photomultiplier signal was amplified fivefold by a low noise preamplifier (300 MHz bandwidth, model SR445; Stanford Research Systems, San Jose, CA) and detected by a dual channel, gated discriminator/photon counter (model SR400; Stanford Research Systems, CA). The discriminator was set at −3 mV for most applications. In some experiments, the signal was processed by a pulse-height analyzer. Photomultiplier signals (10 ns risetime, 25 ns width at half-maximum) were rectified and impedence-matched by a model 113 pre-amplifier (EG & G-Ortec, Oakridge, TN), and then broadened to 2–4 ms width, shaped to a Gaussian waveform, and amplified 250-fold by a model 590A pulse shaper/amplifier (EG & G-Ortec). The signal was processed by a 2048-channel multichannel analyzer (Ace/2K Card; EG & G-Ortec) in an 80387 cpu.

Several measures were taken to minimize electronic noise and signal drift. The instrument components were surrounded by a grounded copper Faraday cage as shown in Fig. 1. The 120-V power lines were filtered by a Weber Line conditioner (model DS6; Chicago, IL). Electrical cables were constructed from dual shielded Belden 9310 cable wire. All components (except for the computer) were placed in a dark room; stray light was further excluded by surrounding the Faraday cage with photographic-grade opaque black cloth (Duvatyne; A. Gasser Inc., San Francisco, CA). The dark room was air conditioned (15 ± 2°C) to reduce photomultiplier temperature and atmospheric moisture.

Cell and lipid membrane preparations

Small unilamellar vesicles containing egg yolk phosphatidylcholine (1 mM for fatty acid exchange studies, 6.4 mM otherwise) and either an anthroyloxy fatty acid (1.3–4 mol%) or ^{3}H-cholesterol (1.8 μM, 80 μCi/ml for fatty acid exchange studies) were prepared by probe sonication (Huang, 1972). Lipids were dried under flowing N_2, hydrated, and briefly vortexed in 2 ml of 66 mM Na phosphate, pH 7.5 (buffer A). The lipid mixture was sonicated at 4°C for 15 min in a model MS-50 Microson cell disruptor (Heat Systems Ultrasonics, Farmingdale, NY) at 60–70% of maximum power. Vesicles were also prepared by extrusion through 0.1 μm polycarbonate filters using a high pressure extruder (Lipex, Canada). Micelles containing oleic acid (1 mM) and an anthroyloxy fatty acid (12-AS, 20 μM) were prepared by addition of 10 μl of an ethanolic solution of the lipids to 3 ml of buffer A while rapidly vortexing.

Erythrocytes were isolated from fresh human blood drawn into isotonic citrate-dextrose. Plasma and white cells (buffy coat) were removed by centrifugation at 1,000 *g* for 5 min; erythrocytes were washed three times with 20 volumes of 10 mM phosphate, 150 mM NaCl (PBS), pH 7.5. For the H_2DIDS binding experiments, cells were washed with PBS, pH 8.0. Sealed white ghosts for transport experiments were prepared by a modification of the method of Bjerrum (1979) in which erythrocytes were lysed at pH 6.0 in 3.8 mM acetic acid, 4 mM $MgSO_4$, washed 4 times in 2 mM phosphate, 1.2 mM sodium acetate, 4 mM $MgSO_4$, pH 7, and resealed by a 45 min incubation in 2 mM Tris, 165 mM KCl, 4 mM $MgSO_4$ at 37°C. Unsealed ghosts for other experiments were prepared by hypotonic lysis of washed erythrocytes using 10 mM sodium phosphate, 1 mM EDTA, pH 8.0 (Dodge et al., 1963).

J774A.1 mouse macrophages (ATCC TIB67) were obtained from the Cell Culture Facility (at UCSF) and grown in suspension culture at 37°C to a density of 4–8 × 10^7 cells/ml in DME medium supplemented with 10% fetal calf serum. The cells were pelleted by centrifugation (250 *g*, 5 min) and resuspended in DME medium for transport experiments.

Fatty acid binding to albumin

Fatty acid binding studies were performed by a modification of the method of Spector and John (1968). The potassium soap of oleic acid (0–4 mM) was prepared by addition of 10 μl of 15 mM KOH to 3 ml of a 0.3 mM stock solution of fatty acid-free BSA in buffer A while rapidly vortexing. These mixtures were non-turbid. After 1 h, the potassium soap of ^{3}H-oleic acid (4 μM final concentration) was added to the oleic acid-BSA mixture while vortexing, and incubated for an additional 1 h to achieve binding equilibrium (Weisiger and Ma, 1987).

H_2DIDS binding to erythrocyte membranes

A stock solution of ^{3}H-H_2DIDS was prepared in water (pH 4) and stored at −20°C. The concentration and purity of ^{3}H-H_2DIDS were checked by absorption spectroscopy (peaks at 273 and 285 nm with extinction coefficient of 34,500 M^{-1} cm^{-1} at 285 nm). Stock solutions of nonradioactive H_2DIDS (5 mM) were prepared freshly in PBS. A solution containing ^{3}H-H_2DIDS (13 μCi/ml) with or without a 200-fold molar excess of unlabeled H_2DIDS was added to washed erythrocytes at 10% hematocrit in PBS, pH 8, and incubated for 30 min at 37°C (Cabantchik and Rothstein, 1974). The ^{3}H-H_2DIDS concentration was chosen to be a fourfold molar excess over the band 3 concentration, estimated assuming 10^5 band 3 monomers per cell and 10^{10} packed erythrocytes per ml. After the 30-min incubation, 30 volumes of ice-cold 10 mM ethylenediamine was added to inactivate unreacted H_2DIDS. The erythrocytes were washed twice with isotonic Tris-buffered saline (pH 8), once with Tris-buffered saline containing 0.5% BSA, and then once with PBS. White ghosts were prepared from these cells and suspended at a concentration of 1.3–1.6 mg protein/ml in lysis buffer for radioluminescence measurements. Incorporated ^{3}H radioactivity was measured by liquid scintillation spectrometry and corrected for ghost protein concentration (Bradford, 1976).

Cell labeling procedures

J774 macrophages (7 × 10^7 cells/ml) were incubated with 10 μM BCECF-AM for 20 min at 37°C. The nonfluorescent BCECF-AM permeates the cells and is hydrolyzed to the impermeant and fluorescent compound BCECF (Dive et al., 1988). After loading, cells were washed once with 5 ml of DME medium. The BCECF-loaded cells contained ~100 μM BCECF in the cytosolic compartment as measured fluorimetrically; the BCECF leakage rate was <15% per h at 22°C. The BCECF-loaded cells were incubated with ^{3}H-*O*-methyl-glucose (0.2 mCi/ml) for 15 min at 22°C for glucose efflux measurements.

Unsealed ghosts (1 mg/ml) were incubated with 5 mM sodium phosphate, 1 mM EDTA, pH 8 containing 5,6-carboxyfluorescein (5 mM) for 10 min on ice. The carboxyfluorescein-loaded ghosts were resealed and washed three times with PBS, pH 8, and incubated at a concentration of 1 mg protein/ml with ^{3}H-D-glucose (0.2 mCi/ml) for 15 min at 22°C before the measurement of glucose efflux (see below). The final concentration of the carboxyfluorescein in a 1 mg/ml suspension of ghosts used for radioluminescence measurements was ~1 mM as determined spectrophotometrically.

Lectin binding procedures

^{3}H-oleic acid-labeled erythrocyte membranes were prepared by a modification of the method of Broring et al. (1989). A solution of ^{3}H-oleic acid (0.2 mCi/ml in ethanol) was injected into washed erythrocytes at 50% hematocrit while rapidly vortexing in a glass test tube and incubated for 5 min at 37°C in PBS containing 11 mM glucose. ^{3}H-oleic acid-labeled ghosts were then prepared from the radioactively labeled erythrocytes by five washes in lysis buffer. The amount of ^{3}H-oleic acid incorporated into the membranes was 40–50 μCi/mg protein (~40% incorporation efficiency).

To label ghosts with fluorescein-wheat germ agglutinin (FL-WGA), the radiolabeled ghosts were resealed in PBS, 2 mM $MgSO_4$, pH 7.5 for 30 min at 37°C, spun, and resuspended at 1.2–1.7 mg/ml protein in 15% dextran (MW 40 kD). These conditions reduced agglutination by FL-WGA without appreciably affecting FL-WGA binding as determined by fluorescence microscopy. 10 nmol of FL-WGA was then added to a 0.5 ml ghost suspension in dextran while rapidly vortexing. SPR measurements were carried out within 2 h. In a control experiment, the radiolabeled ghosts were incubated with a mixture of FL-WGA, *N*-acetylglucosamine (50 mM) and ovomucoid (0.5 mg/ml). After SPR measurements, membranes were washed with PBS and solubilized in 1% SDS for spectrophotometric determination of bound FL-WGA (ϵ_{497} of 5.8 × 10^4 M^{-1} cm^{-1}).

Radioluminescence measurements

A rapid injection method was used for studies of lipid exchange kinetics and membrane transport. Solutions were injected into the sample container through thin teflon tubing (0.8 mm inside diameter) attached to a 21-gauge steel needle which was cemented into the plastic cap so that the needle tip was at the bottom of the container. An outflow port for air exit and sample overflow was provided by a needle whose tip was just below the cap. To initiate solute efflux in transport studies, radioactively labeled cells in the sample vial were diluted rapidly by nonradioactive buffer. The diluting buffer was injected from outside of the dark room.

As described in the accompanying manuscript, quantitative analysis of radioluminescence signals requires corrections for fluorophore quantum yield (Q_y), the photomultiplier quantum efficiency [$Q_e(\lambda)$], the probability that an emitted photon exits the sample vial (inner filter effect, I_a), and the probability that a photon reaches the detector (geometric factor G). Fluorophore quantum yield was determined from integrated corrected emission spectra relative to fluorescein in 0.1 N NaOH (Q_y = 0.92, Weber and Teale, 1957) or quinine sulfate in 0.2 N H_2SO_4 (Q_y = 0.7, Scott et al., 1970), after correction for sample absorbance. $Q_e(\lambda)$ was taken from a polynomial fit to data provided by Thorn-EMI. The inner filter effect correction factor (I_a) was given by,

$$I_a = \int F(\lambda)\, 10^{-d \cdot A(\lambda)}\, d\lambda \Big/ \int F(\lambda)\, d\lambda, \qquad (1)$$

where $A(\lambda)$ is sample absorbance per cm pathlength, $F(\lambda)$ is the fluorophore emission spectrum, and d is the effective pathlength traveled by the photon in the container from its point of origin to the container boundary. The pathlength d was determined experimentally to be 0.40 ± 0.08 cm using aqueous solutions of tryptophan (to give radioluminescence) and sodium nitrite (to give inner filter effect) which absorbs

photons at tryptophan emission wavelengths ($\epsilon_{352} = 28\ M^{-1}\ cm^{-1}$). A Monte Carlo simulation using the geometry of the sample vial gave a consistent d value of 0.41 cm. The probability that a photon reaches the detector (G) is dependent on the geometry of the sample vial and the photon collection optics. A Monte Carlo simulation using the sample vial placement of 45 mm from the photomultiplier cathode and the photomultiplier active surface area of 15.9 cm^2 gave a G factor of 0.035 in the absence of the mirror. From the ratio of the SPR signals obtained with and without the mirror, the G factor was determined to be 0.052 under the conditions of our experiments.

Distance calculations

Explicit equations were developed for approximate calculation of distances for point-to-point and point-to-plane geometries based on the Monte Carlo simulations reported in the accompanying paper (Bicknese et al., 1992). For point-to-point fluorophore-radioisotope geometry, the distance R_0 (cm) is given by,[1]

$$R_0 = [(m\sigma_F A_r n_F)(Q_e Q_y I_a G/L_{rad})]^{0.44}, \quad (2)$$

where m was determined from the Monte Carlo simulation (1.26×10^7 $keV \cdot cm^{-5.25} \cdot \mu Ci^{-1}$ for ^3H), L_{rad} is the SPR signal in cps, A_r is donor radioactivity (μCi), n_F is the number of fluorophores that can serve as acceptors for each donor molecule, and σ_F is the excitation cross-section (excited fluorophore $\cdot$ cm^3 $\cdot$ fluorophore^{-1} $\cdot$ μCi^{-1} $\cdot$ keV^{-1} $\cdot$ s^{-1}) as given in Fig. 4 of the accompanying paper. When ^{14}C is the donor, $m = 4.75 \times 10^6$ ($keV \cdot cm^{-5.25} \cdot \mu Ci^{-1}$).

For a plane of ^3H donors exciting a point fluorophore at perpendicular point-to-plane distance of R_0,

$$R_0 = \{(m\sigma_F n_F \rho_r)(I_a Q_y G Q_e)/ [L_{rad} - b(\sigma_F n_F \rho_r)(I_a Q_y G Q_e)]\}^{\xi}, \quad (3)$$

where $m = 1.73 \times 10^7$ ($keV \cdot cm^{-(1+1/\xi)} \cdot \mu Ci^{-1}$), $b = -3.04 \times 10^8$ ($keV \cdot cm^{-1} \cdot \mu Ci^{-1}$), ξ is an empirically derived dimensionless exponent = 3.17, ρ_A is the donor density in the plane ($\mu Ci \cdot cm^{-2}$), n_F is the number of fluorophore accessible to the donor radioisotope, and σ_F is as defined above. For ^{14}C, $m = 2.05 \times 10^4$ ($keV \cdot cm^{-(1+1/\xi)} \cdot \mu Ci^{-1}$), $b = 8.42 \times 10^7$ ($keV \cdot cm^{-1} \cdot \mu Ci^{-1}$), and $\xi = 1.15$.

[1] From the accompanying paper, $L_{rad} = N^*[S(R)]I_a(\lambda)Q_y G Q_e(\lambda)$, where L_{rad} is the measured SPR signal, $N^*[S(R)]$ is the theoretical SPR signal, and $I_a(\lambda)$, Q_y, G, and $Q_e(\lambda)$ are corrections for inner-filter effect, fluorophore quantum yield, geometric factor, and photomultiplier quantum efficiency, respectively. For point-to-point donor-acceptor geometry, $N^*[S(R)] = \sigma_F A_r n_F D'_x(R_0)$, where σ_F is the corrected fluorophore cross-section, A_r is radioactivity in μCi, n_F is the number of fluorophores associated with each radioisotope, and $D'_x(R_0)$ is the energy density distribution of the beta decay. For point-to-plane or plane-to-plane acceptor-donor geometry, $N^*[S(R)] = \sigma_F n_F \rho_r D_p(R_0)$, where n_F is the number of fluorophores, ρ_r is the radioisotope density in the plane, and $D_p(R_0)$ is the energy density distribution. When the radioisotope is the point and the fluorophores are distributed in the plane, $N^*[S(R)] = \sigma_F \rho_F A_r D_p(R_0)$. $D'_x(R_0)$ and $D'_p(R_0)$ were related empirically to R_0 by $D'(R_0) = mR^{(-1/\xi)} + b$ and the parameters m, b, and ξ were determined by a regression. Substitution of the L_{rad} and $N^*[S(R)]$ expressions into this empirical equation gives Eqs. 2 and 3 in the text.

[2] From the data given in Fig. 4 A, the SPR signal is linearly dependent on the radioactivity. Thus, for excitation of albumin tryptophans by bound ^3H-OA ligands, L_{rad} is proportional to the albumin-bound ^3H-OA concentration, $[OA_b^*]$: $L_{rad} = \alpha[OA_b^*]$, where α is a scaling factor. Binding equilibria among albumin, OA*, and nonradioactive OA with a dissociation constant (K_d) is,

$$OA_b \overset{K_d}{\underset{OA}{\rightleftharpoons}} BSA \overset{K_d}{\underset{OA^*}{\rightleftharpoons}} OA_b^*.$$

For n independent long chain fatty acid binding sites per albumin, each of equal affinity, K_d is given by,

$$K_d = n[P_f][OA_f]/[OA_b] = n[P_f][OA_f^*]/[OA_b^*]$$

where $[P_t]$ is the albumin concentration, and subscripts f and b denote free and bound ligand, respectively. The mass-balance relations are,

$$[OA_t] = [OA_f] + [OA_b], \quad [OA_t^*] = [OA_f^*] + [OA_b^*], \quad \text{and}$$
$$n[P_t] = n[P_f] + [OA_b^*] + [OA_b].$$

Substituting the mass-balance relations into the expressions for K_d and L_{rad} gives,

$$L_{rad} = \alpha[OA_t^*]/2[OA_t] \times \{x - \{x^2 - 4(n[P_t][OA_t] - L_{rad}[OA_t]/\alpha)^{0.5}\}\},$$

where $x = (-L_{rad}/\alpha + [OA_t] + n[P_t] + K_d)$. Using $K_d = 10^{-7}\ M^{-1}$, a nonlinear regression of L_{rad}, $[OA_t^*]$, and $[OA_t]$ provided the parameters n and α.

RESULTS

Instrument performance

To minimize background drift for measurement of very low radioluminescence signals, a gated detection mode was used in which background signal was subtracted continuously. The principle of gated detection as applied here is shown in Fig. 2 A. Signal A (sample plus background) was collected into photon counter channel A over a gating time τ, during which time the detector was unoccluded. Signal B (background) was collected into channel B for an equal time τ, during which time the detector was completely occluded. The background-subtracted A minus B signal is thus corrected for background drift. Fig. 2 B shows the A, B and A-B signals as a function of τ for a 608-ms chopper rotation period. The A and A-B signals increased linearly with τ until τ was close to the half period of the chopper; for larger τ, the open and closed signals overlapped. From these data, τ was chosen to be 225 ms for subsequent experiments. Fig. 2 C shows a representative signal profile from a miceller sample containing 22 μCi ^3H-palmitic acid and 2 μM 12-AS. Note that the fluctuations are symmetrical in the A-B signal. The sensitivity and linearity of the photon counting instrument were assessed using ^3H-glucose in scintillation fluid. Fig. 2 D shows excellent linearity of the A-B signal over a 1,000-fold signal range. For a 30-min data acquisition, a radioluminescence signal of 1.3 ± 0.4 cps (SE) was measurable.

The gated signal detection method above makes use of a single discriminator setting to reject low amplitude pulses which consist predominantly of electronic noise. High amplitude noise and spurious signals cannot be rejected by a single discriminator setting. To evaluate the spectrum of signal amplitudes, pulse-height analysis was performed by a multichannel analyzer. Fig. 3 shows representative pulse height distributions which have been

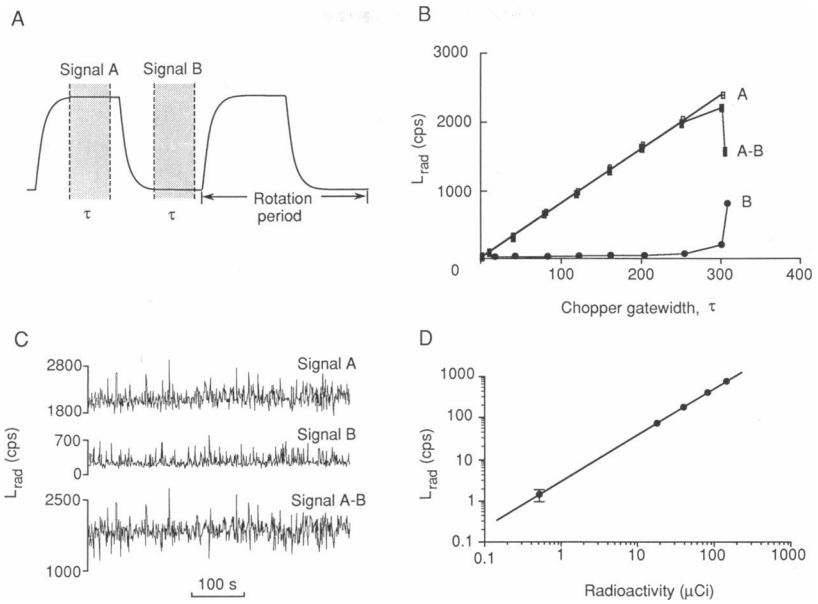

FIGURE 2 Radioluminescence measurement by gated photon counting. (*A*) Gated pulse profiles. Signals A and B are collected during the indicated interval τ in the open gate and the closed gate, respectively. See text for details. (*B*) Amplitudes of the signals A, B, and A-B as a function of gatewidth τ. (*C*) Time course of radioluminescence signal for a sample consisting of 22 μCi ^{3}H-palmitic acid and 2 μM 12-AS micelles in water. Each point represents the integrated signal over 1 s. (*D*) Linearity of the radioluminescence signal (mean ± SE) with amount of ^{3}H-glucose in scintillation fluid. Data acquisition times varied from 30 min (0.3 μCi) to 10 s (100 μCi). The fitted line has slope 0.98 and correlation coefficient 0.9996.

normalized to give identical areas. The low amplitude signal (<1 mV, channels 0–90) consists of electronic noise. The high amplitude signal (>20 mV, channels > 2,000) arises, in part, from electronic noise and cosmic rays which produce Cerenkov radiation in the quartz photomultiplier window. The broad central peak arises primarily from the photons produced by radioluminescence (profiles *B–D*), and thermal electrons generated at the cathode in the dark (dark noise, profile *A*). The width of the pulse height distribution is determined by statistical fluctuations in the number of photoelectrons produced mainly by the first dynode.

Multichannel analysis allows in principle the distinction between single photon and multiple photon events. The appearance of multiple photons at the photomultiplier surface within the coincidence time (~20 ns) would give signals with higher amplitudes. An example of a multiple photon event is shown in profile *D*. Excitation in a scintillation fluid by ^{3}H-glucose gave a pulse height distribution that is remarkably broadened compared with those obtained for SPR signals. Note that the single photon SPR signals from fluorophores in the 280 to 600 nm range are not distinguishable by multichannel analysis since the difference in their emission photon energies (<3 eV) is too small to alter the number of photoelectrons produced at the first dynode. For subsequent measurements of radioluminescence by pulse height analysis, signals from channels 90 to 1104 were integrated (see stippled bar above abscissa). Fig. 3 (*Inset*) shows the stability of the integrated signal measured by multichannel analysis over a 12-h period. The dark counts (*filled circles*) increased gradually, but the sample signal (*open circles*) remained constant over time.

Measurements in homogeneous solutions

Fig. 4 *A* shows the dependence of Bremsstralung (stopping radiation) and a radioluminescence signal (fluorescein excitation by ^{3}H) on the amount of radioisotope. As predicted by the theory in the accompanying manuscript (Bicknese et al., 1992), signals increased linearly with the amount of radioisotope. Fig. 4 *B* shows that at a constant amount of radioactivity, the SPR signal increases linearly with the concentration of fluorophore. These results are consistent with the radioluminescence theory and demonstrate the linearity of the detection system.

Effect of sample turbidity on SPR signal

An important concern for SPR measurements in cellular and membrane samples is the effect of light scattering due to sample turbidity. To investigate effects of turbidity, the SPR signal from ^{3}H-glucose (20 μCi) and tryptophan (1 mM) was measured in the presence of PC liposomes which strongly scatter light. Interestingly, the SPR signal (14.5 ± 0.5 cps) was not affected significantly at the highest concentration of liposomes used (1.2 mM PC; 13.3 ± 0.6 cps) in which the OD (1 cm) at the tryptophan emission wavelength of 340 nm was 8.8. Further,

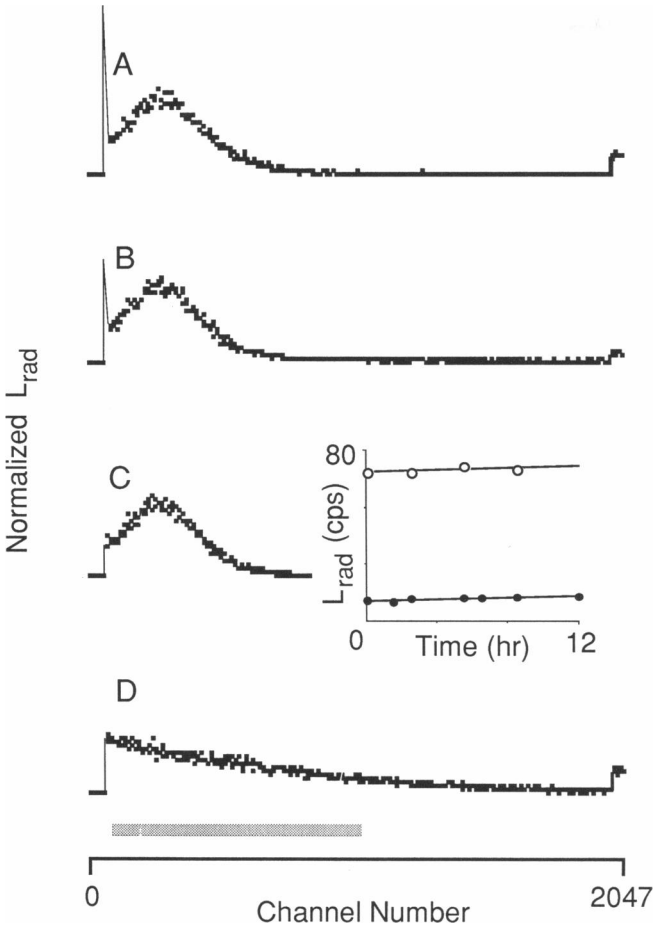

FIGURE 3 Radioluminescence measurement by pulse height analysis. Representative pulse height distributions of photomultiplier dark noise (*A*), aqueous solutions of 10 μCi ^{3}H-glucose and 12 mM tryptophan (*B*) or 10 mM fluorescein (*C*), and 10 μCi ^{3}H-glucose in scintillation fluid (*D*). The range of pulse heights used for signal integration is shown by the stippled bar. (*Inset*) Instrument stability over a 12-h period. Data shown are the integrated signals from photomultiplier dark noise, and a sample consisting of ^{3}H-glucose and 10 mM tryptophan. Individual points were determined from the time required for acquisition of 3,000 counts.

the addition of white erythrocyte ghost membranes up to a concentration of 1.6 mg protein/ml (OD_{340} = 4.8, 1-cm pathlength) had little effect on the SPR signal (16.0 ± 1.0 cps). These findings indicate that elastically scattered light from turbid biological samples is efficiently collected with no measurable effect on the SPR signal. The lack of effect of turbidity on radioluminescence measurements facilitates experiments performed at high membrane concentrations. It is important to reiterate that inelastically scattered light (inner filter effect) does attenuate the SPR signal as described in Experimental Methods.

Effect of fluorophore environment on SPR signal

Solvent "scintillation," defined as the enhancement of fluorophore excitation by energy transfer from the solvent, has been reported for aromatic and hydrocarbon solvents (Hirayama and Lipsky, 1971). Although radioluminescence measurements in biological samples are performed in an aqueous environment where no scintillation is expected, the microenvironment of the fluorophores might consist of lipid, carbohydrate, or protein. Thus, for quantitative interpretation of SPR signals, it is important to evaluate possible scintillation effects of phospholipids, proteins, and carbohydrates in the vicinity of the fluorophore acceptor. Previous studies have shown that the presence of electronegative atoms such as oxygen in a solvent decreases its ability to act as a scintillant (Hirayama and Lipsky, 1971), suggesting that phospholipids, carbohydrates and proteins should be poor scintillants.

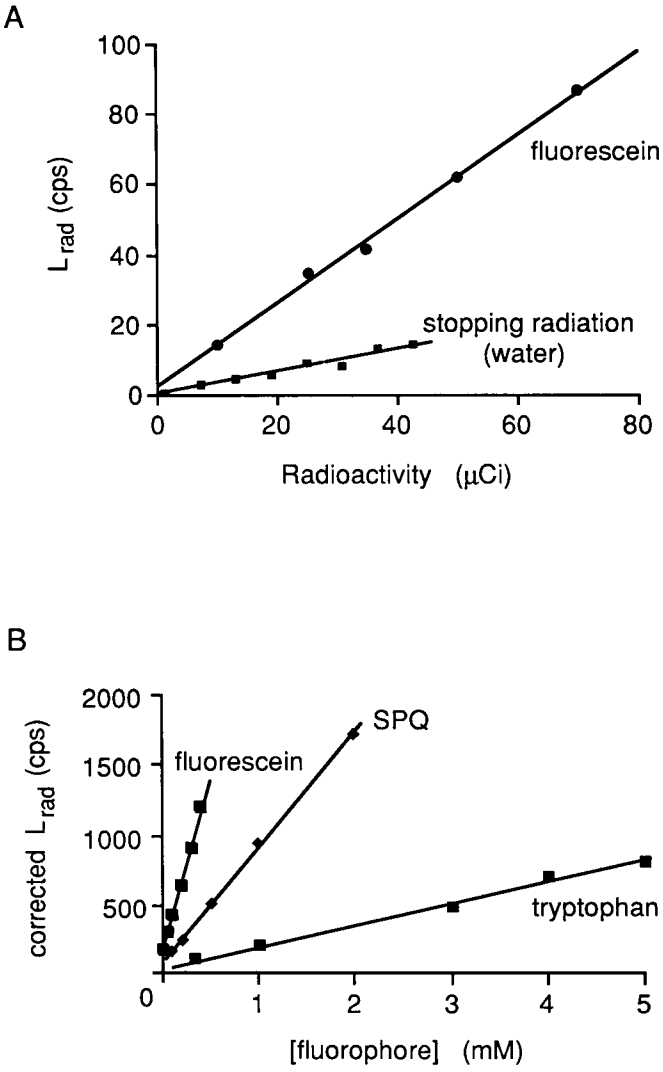

FIGURE 4 Dependence of radioluminescence signal on radioisotope and fluorophore concentrations. (*A*) Samples contained various amounts of ^{3}H-glucose in water or a pH 8 buffer containing 100 μM fluorescein. (*B*) Samples contained 10 μCi ^{3}H-glucose in water containing various concentrations of tryptophan, SPQ and fluorescein. Signals were determined by integration of the pulse height distributions and corrected for inner filter effect.

Effects of protein and carbohydrate microenvironments on SPR signals were evaluated by comparison of the SPR signal from fluorescein in solution (66 mM Na phosphate, pH 8.0) with that bound to proteins or carbohydrates in the same buffer. For these measurements, a KV 450 cut-on filter was placed between the sample and the photomultiplier to eliminate the signal from tryptophans and to decrease the contribution from Bremsstrahlung. The signal from samples containing 20 μCi ^{3}H-glucose and 50–100 μM fluorescein-IgG, WGA, and dextran were each comparable to that of fluorescein alone (Table 1) after corrections for quantum yields, inner filter effect, photomultiplier efficiency, and sample absorbance. These results indicate absence of scintillant effects in protein and carbohydrate microenvironments.

Effect of lipid environment was evaluated by measurement of SPR signals from PC vesicles containing fatty acids labeled with the anthroyloxy chromophore at different positions along the acyl chain. The anthroyloxy chromophore resides at specified depths in the lipid bilayer (Thulborn and Sawyer, 1978). The SPR signal from PC vesicles containing 1.3 mol% anthroyloxy stearic acid did not appreciably change with increasing depth of the chromophore into the bilayer (Table 2). However, the AS fatty acids dissolved in ethanol gave an SPR signal ~20% lower than that in vesicles, indicating that the efficiency of excitation of anthroyloxy fluorescence is enhanced by incorporation into the lipid bilayer. These findings suggest that labeling of the hydrophobic region of membranes with a fluorophore acceptor for quantitative SPR distance measurement should be made with caution. In contrast, membrane labeling with the radioactive donor would not have any uncertainty associated with the scintillant effect.

Fatty acid transfer in model membranes

The transfer of fatty acids from vesicles or micelles to vesicles was measured from the radioluminescence which appears when a radioactive donor and a fluorophore acceptor are in close proximity. Fatty acid exchange between lipid vesicles has been studied by fluorescence resonance energy transfer (Storch and Kleinfeld, 1986); an advantage of the radioluminescence approach is that fluorescent labeling of lipid molecules is not required.

The transfer of 12-AS from sonicated PC vesicles to vesicles containing ^{3}H-cholesterol was measured by a rapid injection method. It is known that the half-time for exchange of cholesterol between vesicles is ~2 h (Lund-Katz et al., 1988), much slower than that of fatty acids. Fig. 5 *A* shows the time course of increasing SPR signal as 12-AS is transferred from nonradioactive to radioactive vesicles. The transfer of 12-AS from oleic acid micelles to sonicated vesicles at 22°C (Fig. 5 *B*) was much faster than that from vesicle to vesicle (Fig. 5 *A*). At a lower temperature of 17°C, the micelles became turbid because of formation of aggregated lamellar structures, giving a much slower rate for 12-AS transfer to PC vesicles (Fig. 5 *C*). The time constants for biexponential fits to the data were 1.9 min (preexponential factor, 0.34), 9.8 min (0.66) for vesicle-to-vesicle transfer and 0.6 min (0.55), 11.7 min (0.45) for micelle-to-vesicle transfer at 22°C; at 17°C, a single time constant of 25.3 min was obtained.

TABLE 1 Effect of the protein and carbohydrate environment in the vicinity of the fluorophore on SPR signal

	Q_y	L_{rad}
		cps
FL (unconjugated)	0.76	75 ± 8
FL-IgG	0.73	81 ± 8
FL-WGA	0.23	76 ± 8
FL-dextran	0.66	70 ± 7

Samples contained 20 μCi ^{3}H-glucose and the indicated proteins (IgG and WGA) and carbohydrate (dextran), covalently conjugated to fluorescein in buffer A (see Methods). The background-subtracted signal (L_{rad}) was corrected for I_a and sample absorbance, and normalized to the Q_y (0.76) and Q_e (10.8%) of unconjugated fluorescein. Data are mean ± SE for 2 sets of measurements.

TABLE 2 Effect of lipid environment in the vicinity of the fluorophore on SPR signal

	Ethanol		PC vesicles	
Fluor	Q_y	L_{rad}	Q_y	L_{rad}
2-AS	0.22	36 ± 6	0.49	47 ± 5
6-AS	0.21	39 ± 6	0.55	53 ± 6
9-AS	0.21	40 ± 4	0.58	53 ± 5
12-AS	0.22	46 ± 8	0.72	51 ± 5

Samples contained 80 μM anthroyloxy stearic acid incorporated into egg PC vesicles (6.4 mM in buffer A) or dispersed in ethanol in the presence of 8 μCi ^{14}C-urea. The background-subtracted SPR signal was corrected for I_a and sample absorbance, and normalized to the Q_y (0.49) and Q_e (18.1%) of 2-AS in vesicles. The data are mean ± SE of 2 sets of experiments.

Fatty acid-albumin binding

The binding of a radioactive ligand to its site on a protein or lipid membrane can be measured by radioluminescence. For ligand binding to a protein, intrinsic protein tyrosines and tryptophans can be used as the fluorescent acceptor. SPR signals could be potentially enhanced by protein labeling with additional chromophores that have higher molar extinction coefficients and quantum yields.

Because of its importance in metabolism, ligand binding to bovine serum albumin has been studied extensively. Long chain fatty acids bind to albumin at high and low affinity sites (Kragh-Hansen, 1989). Bovine serum albumin has 15 tyrosines and 2 tryptophans (Hirayama et al., 1990) that are in close proximity to the

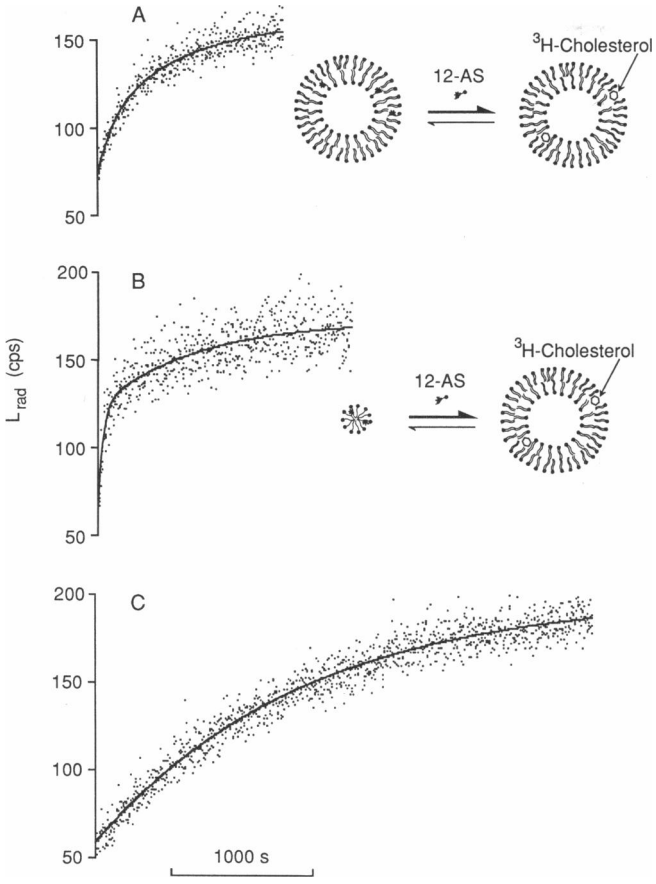

FIGURE 5 Measurement of fatty acid exchange kinetics in lipid membranes by SPR. (*A*) Transfer of 12-AS (20 μM) from sonicated PC vesicles (0.5 mM) to sonicated PC vesicles (0.5 mM) containing 40 μCi ^{3}H-cholesterol. The reaction was initiated by rapid mixing and counts were accumulated in 3-s intervals. Data are the averages of 3 measurements. The parameters for fitted biexponential curves are given in the text. (*B* and *C*) Transfer of 12-AS (20 μM) from oleic acid micelles (0.5 mM) to PC vesicles containing ^{3}H-cholesterol at 22°C (*B*) and 17°C (*C*).

fatty acid binding domains (Brown and Schockley, 1982; Cistola et al., 1987) and can serve as potential fluorescent acceptors in a radioluminescence experiment. The binding of ^{3}H-oleic acid to fatty acid-free BSA was examined in the presence of increasing amounts of nonradioactive oleic acid. Fig. 6 *A* shows a radioluminescence signal of 13 ± 2 cps (SE, n = 3) in the absence of unlabeled oleic acid which remained nearly constant up to a ~3:1 molar stoichiometry of unlabeled oleic acid to albumin. The SPR signal then decreased to near background at higher concentrations of unlabeled oleic acid. Background signal, consisting of photomultiplier dark counts and Bremsstrahlung (~26 cps) was subtracted, so that the plotted radioluminescence signal correspond to the albumin fluorescence that was excited by ^{3}H-oleic acid.

The relationship between L_{rad} and the concentration of unlabeled oleic acid provides information about the stoichiometry of oleic acid binding to albumin. Assuming a single class of high affinity saturable binding sites under the conditions of this experiment, the data were fitted to a binding model as described in footnote 2. The fitted curve in Fig. 6 *A* gives a stoichiometry of 2.7 ± 0.3 oleic acid binding sites per albumin, in agreement with the published value of 3.

Binding of ^{3}H-H_2DIDS to erythrocyte band 3

The binding of the stilbene inhibitor ^{3}H-H_2DIDS to its site on the erythrocyte anion transporter, band 3 (Cabantchick and Rothstein, 1974; Lepke et al., 1976) was measured by SPR. In intact erythrocytes, H_2DIDS binds primarily to the 60-kD membrane spanning domain of band 3 which contains 7 tryptophans (Tanner et al., 1988). Ghost membranes were prepared from erythrocytes labeled with ^{3}H-H_2DIDS in the absence or presence of a 200-fold molar excess of unlabeled H_2DIDS; the difference was taken to be the specific binding of ^{3}H-H_2DIDS to band 3 (Cabantchik and Rothstein, 1974). In three sets of experiments, a range of 0.31–1.5 × 10^6 sites per erythrocyte were labeled with ^{3}H-H_2DIDS as determined from ghost radioactivity, protein concentration, ^{3}H-H_2DIDS specific activity, and ghost band 3 content (25% of membrane proteins, 10^5 copies per ghost). Fig. 6 *B* shows that the SPR signal from ghosts (0.78 mg protein) was 4.0 ± 0.6 (SE, n = 2) cps for 1 μCi bound ^{3}H-H_2DIDS after subtraction of the background signal from buffer alone. Control experiments were performed to show that this signal was due to specific binding of ^{3}H-H_2DIDS to the membranes. The addition of excess unlabeled H_2DIDS inhibited ^{3}H-H_2DIDS binding by up to 80% and reduced the radioluminescence signal. Also, the SPR signal from ghosts containing ^3H_2O in an amount equivalent to the ^{3}H-H_2DIDS radioactivity bound to ghosts was not significantly greater than the signal from ghosts alone (Fig. 6 *B*).

Membrane transport measurements by SPR

The transport of solute molecules across cell membranes is of central importance for cell metabolism and for carrying out specialized functions such as salt secretion in epithelial cells. All cells contain glucose transporters that carry glucose from the external environment to the cell interior for metabolic processing (Wheeler and Hinkle, 1985). The SPR method was used to measure the kinetics of solute transport in real time and without the need to physically separate cells from external solute.

The transport of a nonmetabolizable sugar, ^{3}H-3-*O*-methyl-glucose (3-OMG) across the plasma membrane of J774 macrophages was studied. Macrophages were labeled with the fluorescent indicator BCECF to serve as the acceptor for intracellular 3-OMG. BCECF-labeled cells were loaded with 3-OMG and diluted with an excess of nonradioactive buffer to initiate 3-OMG efflux. Fig. 7 *A* (*bottom curve*) shows the time course of decreas-

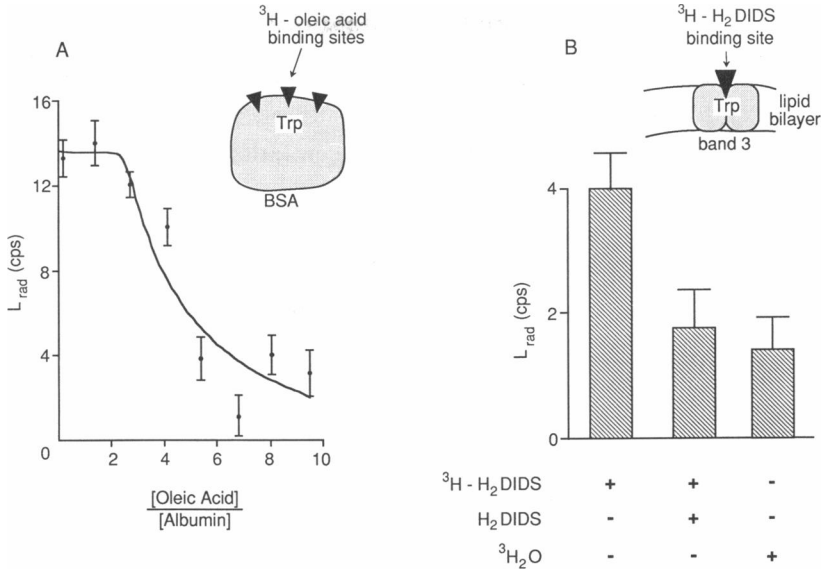

FIGURE 6 Detection of ligand binding by SPR. (*A*) Binding of ^{3}H-oleic acid to BSA in the presence of increasing concentrations of non-radioactive oleic acid. Samples contained 0.3 mM BSA, 5 μCi ^{3}H-oleic acid, and varying concentrations of unlabeled oleic acid. Data are the mean ± SE of 3 sets of independent measurements obtained after subtraction of background signal (see text). The fitted curve was obtained for a single site saturable binding model with a stoichiometry of 2.7 oleic acid binding sites per albumin. (*B*) Binding of ^{3}H-H_2DIDS to erythrocyte membranes. Samples contained 1.5 mg/ml ghosts prepared from unlabeled erythrocytes, and erythrocytes labeled with ^{3}H-H_2DIDS (1 μCi) in the presence or absence of excess unlabeled H_2DIDS. In addition, the signal from unlabeled ghosts containing 1 μCi ^3H_2O is given. Data are mean and SE of 2–3 sets of independent measurements after subtraction of the background signal obtained with buffer alone.

ing SPR signal as the 3-OMG exits the cell. The data were fitted to a single exponential function with a time constant of 81 ± 5 s (n = 2), corresponding to a permeability coefficient of 0.5×10^{-5} cm/s (macrophage surface-to-volume ratio taken to be 2.4×10^3 cm^{-1}). In a parallel experiment, 3-OMG efflux was measured by a rapid filtration technique as shown by the open circles. The efflux rates measured by radioluminescence and rapid filtration were in quantitative agreement. Fig. 7 *A* also demonstrates that the rate of 3-OMG efflux decreases with increasing concentrations of the glucose transport inhibitor, cytochalasin B (Jung and Rampal, 1977). The exponential time constants were 6.3 min and 25 min at cytochalasin B concentrations of 1 and 20 μM, corresponding to 79 and 94% inhibition, respectively. The SPR signal of 147 cps at 0 time (before efflux), measured at a total sample ^{3}H radioactivity of 100 μCi and BCECF concentration of 100 μM, is in agreement with the value of 122 cps predicted from the fluorescein data in Fig. 4 *A*.

For comparison, the transport of ^{3}H-D-glucose in sealed red cell ghosts was measured (Fig. 7 *B*). Ghosts were labeled with 6-CF before sealing as described in Experimental Methods. The half-time for ^{3}H-D-glucose efflux from ghosts was 15.9 ± 0.8 s, corresponding to a permeability coefficient of 0.35×10^{-5} cm/s, similar to that determined in macrophages, and consistent with published data (Jung et al., 1971). In addition, glucose transport in red cell ghosts was strongly inhibited by 20 μM cytochalasin B (Fig. 7 *B*).

Distance between the erythrocyte membrane glycocalyx and the lipid bilayer

The distance between the lectin binding site of the erythrocyte glycocalyx and the membrane lipid bilayer was investigated by SPR. The erythrocyte glycocalyx contains sites for blood group determinants, viral receptors, and plant lectins (Halbhuber et al., 1990; Viitala and Jarnefelt, 1985). It consists primarily of branched chain carbohydrates on glycophorins, band 3, and glycolipids. To measure the distance between the glycocalyx and the lipid bilayer, ^{3}H-oleic acid was used as the lipid bilayer donor label, and fluorescein-wheat germ agglutinin (FL-WGA), which has a higher specificity for glycophorins than for band 3 (Adair and Kornfield, 1974; Lovrien and Anderson, 1980; Danilov and Cohen, 1989), as the glycocalyx acceptor label. The SPR signal from 26.6 μCi ^{3}H-oleic acid-labeled ghosts (0.85 mg protein) and 10.5 μM bound FL-WGA was 5.7 ± 0.5 cps (SE, n = 4) (Fig. 8 *A*). This signal was due to the proximity of the membrane-bound FL-WGA and ^{3}H-oleic acid because: (*a*) disruption of the geometric proximity of the acceptor FL-WGA and the donor ^{3}H-oleic acid by 1% SDS decreased the SPR signal to background, and (*b*) FL-WGA-labeled membranes containing dispersed ^3H_2O of equivalent radioactivity in place of bound ^{3}H-oleic acid had a signal similar to that of nonfluorescent ^{3}H-oleic acid-labeled membranes. Further, the SPR signal was proportional to the amount of bound FL-WGA: compe-

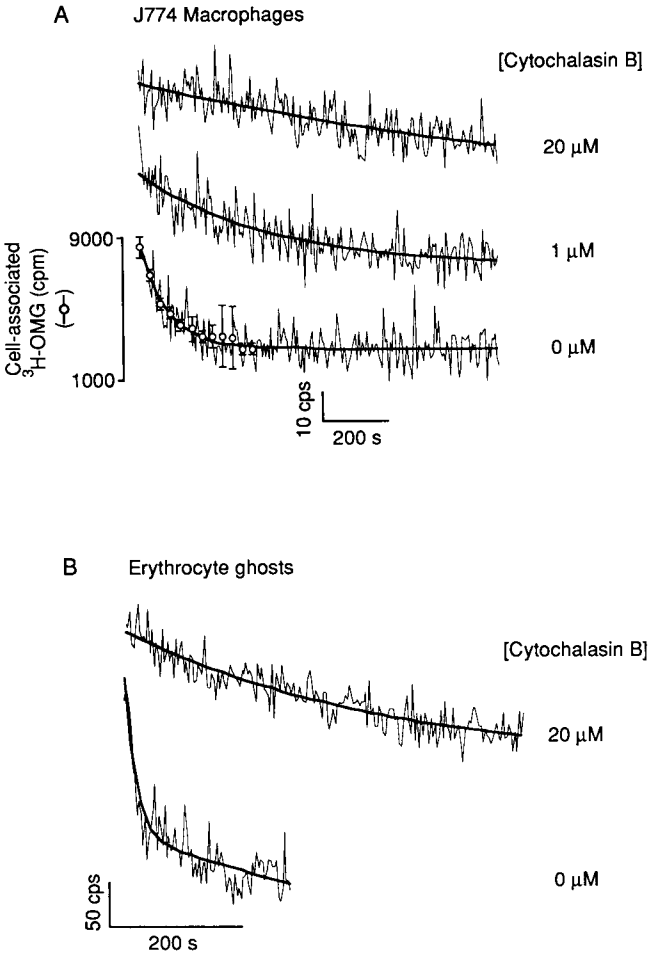

FIGURE 7 Measurement of membrane transport by SPR. (*A*) Efflux of ^{3}H-*O*-methyl-glucose from BCECF-loaded J774 macrophages upon 15-fold dilution of 40 μl of a cell suspension (5×10^7 cells/ml) with nonradioactive buffer in the presence of indicated concentrations of cytochalasin B. The open circles (mean ± SE, $n = 2$) were determined by an efflux-filtration assay in which ^{3}H-OMG-loaded macrophages were diluted with nonradioactive buffer; remaining intracellular radioactivity was measured at the indicated times. (*B*) Efflux of ^{3}H-D-glucose from carboxyfluorescein-loaded erythrocyte ghosts upon a 15-fold dilution with nonradioactive buffer in the absence and presence of 20 μM cytochalasin B. Fitted curves were obtained for exponential regressions.

tition for WGA binding by 0.5 mg/ml ovomucoid and 50 mM *N*-acetylglucosamine (Ivatt et al., 1986) reduced the SPR signal to 1.9 ± 0.2 cps (66% decrease), consistent with the residual 4.2 μM FL-WGA (75% decrease) that remained bound to the membranes as measured fluorimetrically.

Using Eq. 3 for point-to-plane geometry, the amount of bound ^{3}H-oleic acid (26.6 μCi), and a measured quantum yield of 0.23, the SPR signal of 5.7 cps from 10.5 μM bound FL-WGA gave a 5-nm distance between the average position of FL-WGA to the outer bilayer leaflet of the membrane bilayer. This value is consistent with current views of the molecular architecture of the bilayer surface as depicted in Fig. 8 *B* (Viitala and Jarnefelt, 1985; Halbhuber et al., 1990). Confirmation of this distance by fluorescence energy transfer measurements was not feasible because of the high K_d of FL-WGA, giving <2% FL-WGA binding to membranes at sample concentrations required for energy transfer measurements.

DISCUSSION

The purpose of this and the accompanying paper was to establish the theory and detection methods for single

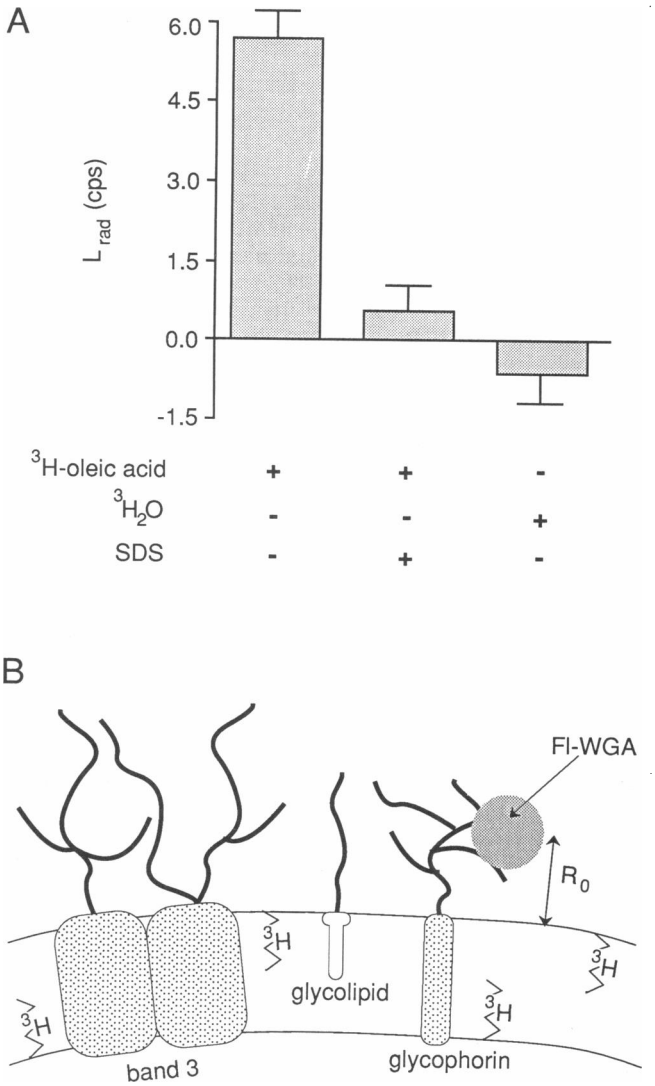

FIGURE 8 Measurement of the distance between the erythrocyte membrane bilayer and glycocalyx by SPR. (*A*) Samples contained erythrocyte ghost membranes (0.8 mg protein), 10.5 μM bound fluorescein-WGA, and 26.6 μCi of bound ^{3}H-oleic acid or dispersed ^3H_2O. Data are mean and SE for 2–4 sets of measurements after subtraction of appropriate background (^{3}H-OA-labeled membranes or ^3H_2O plus membranes). (*B*) Schematic of the erythrocyte membrane glycocalyx showing carbohydrate moieties of glycophorins, band 3, and glycolipids. R_0 is the average distance between the WGA binding sites and the outer leaflet surface.

photon radioluminescence (SPR), and to apply SPR to several biological problems including lipid exchange kinetics, ligand binding, membrane transport, and submicroscopic distance determination. The SPR method makes use of the energy carried by an electron produced by beta decay to excite a reporter fluorescent molecule within the range of the electron. The data demonstrate the feasibility of making SPR measurements on turbid biological samples containing proteins and lipids. Measurements of lipid exchange kinetics, ligand binding and membrane transport can be made in real-time and without the need to separate ligand from receptor or cells. In addition, because the donor ligand molecule is radioactively labeled, it is not necessary to derivatize the native ligand which would potentially alter its function. For distance measurements, the SPR method remarkably extends the distances measurable by fluorescence resonance energy transfer (<10 nm) to >100 nm with ^{3}H, and even further with radioisotopes (^{14}C and ^{35}S) having higher electron energy.

The detection of single photon radioluminescence signals requires a cooled, low noise, and high sensitivity photomultiplier and photon counting electronics. Because of the small SPR signals in some applications requiring long data acquisition times, extensive electrical shielding, light shielding and room temperature control were necessary. In addition, it was necessary to use a mechanical light chopper and a gated detection mode and/or pulse height analysis to correct for background drift and to reject electrical noise. The instrumentation described here can reliably measure ~1 cps above photomultiplier dark counts (9–12 cps) with a 30-min data acquisition. Further improvements in instrument performance should be possible; for example, a high gain, liquid N_2-cooled photomultiplier, as used in astrophysical measurements and high energy physics detectors, may reduce dark counts by up to a factor of 10. Thus, the ultimate practical instrument sensitivity for a long data acquisition is probably <0.1 cps. In addition, replacement of this sample holder and spherical reflector (efficiency ~5%) by a large elliptical mirror with sample and photomultiplier surface at the focal points should increase the light collection efficiency by ~10-fold (Bicknese and Maestre, 1987). From the model reported in the accompanying manuscript, a 0.1 cps signal (and a G factor of 0.5) is expected for a sample containing 1 μCi ^{3}H, with only 1 fluorophore associated with each ^{3}H, where individual fluorophore-^{3}H pairs are separated by a distance of ~30 nm for fluorescein, ~50 nm for rhodamine 6G, and ~400 nm for β-phycoerythrin. In a point-to-plane geometry with a ^{3}H surface density of 10^{-2} μCi/cm^2 and 1 μM fluorophore, the measurable distance is increased to ~800 nm for fluorescein.

The fundamental difference in detection of single photon (SPR) and multi-photon (scintillation spectroscopy) signals is the ability to use a coincidence detection mode in the latter. In principle, the Bremsstrahlung accompanying individual beta decays could be used as a gating signal to accept or reject a signal arriving from radioluminescence. However, the low Bremsstrahlung signal in the spectral range detectable by the photomultiplier makes a gated detection mode for SPR extremely inefficient.

The lack of dependence of SPR signal on elastic light scattering was an interesting observation making possible the use of very turbid samples which are generally not suitable for optical studies. Further, because of the substantial Stoke's shift between the absorption and emission bands of many fluorophores, very high fluorophore concentrations can be used with minimal inner filter effect. Unlike conventional fluorescence measurements, SPR measurements do not require photon excitation so that inner filter effect arises only from absorption of emitted photons. The main concern for quantitative distance measurement by SPR is accurate knowledge of the cross-section for fluorophore excitation. A potentially important factor which introduces uncertainty in the cross-section is the scintillant effect. Although no scintillant effect was observed for a fluorophore bound covalently to proteins and carbohydrates, there was a small increase in radioluminescence when the fluorophore was embedded in the membrane phospholipid domain. It is thus important to recognize the possibility of scintillant effect in the design and interpretation of the SPR measurements. When quantitative distance measurements are not important, the scintillant effect can be used to increase SPR signal intensity.

A diverse group of biological questions were addressed to evaluate several novel applications of SPR. One class of applications which does not require distance determination is the kinetics of transfer of a radioactively-labeled ligand between compartments. Fatty acid transfer between lipid vesicles and glucose transport across cell membranes were chosen as examples. The rates of transfer of anthroyloxy fatty acids were within the range reported by the energy transfer method. The rate of 3-OMG transport across the macrophage plasma membrane was in quantitative agreement with the results of a filtration assay. Importantly, kinetic measurements were made with SPR in real-time and without the need to separate membrane-bound and unbound compartments, and with a radioactive solute rather than chemically modified solute containing bulky fluorescent groups.

SPR has applications to the steady-state measurement of ligand binding. The studies of oleic acid-albumin binding and ^{3}H-H_2DIDS-band 3 binding demonstrate the use of endogenous tryptophans as the fluorescent acceptor. The finding of 3 high affinity oleic acid sites per albumin molecule is consistent with known structural and biochemical data. Improved SPR signals in ligand binding studies would require ligands with increased specific activity, proteins labeled with fluorophores having improved molar absorbance and quantum yield, or de-

creased distance between the radioactive donor and fluorescent acceptor.

An important application of SPR is the measurement of submicroscopic distances that are too large to measure by fluorescence energy transfer. A fundamental difference in the dependence of signals on distance (for point-to-point geometry) is that efficiency for fluorescence energy transfer decreases as R^{-6} at distances exceeding the Forster distance (typically 4–6 nm), whereas the efficiency for radioluminescence decreases as $\sim R^{-2}$. With suitable radioactive donor and fluorescent acceptor molecules, distances of up to 500 nm should be measurable with ^3H. The theory developed in the accompanying manuscript indicates that an absolute distance can be calculated for specified donor-acceptor geometries and amounts of radioactive donor and fluorophore acceptor. The erythrocyte glycocalyx-to-bilayer distance of 5 nm was within the range expected from glycocalyx protein biochemistry and suggested that the carbohydrates of erythrocyte glycophorins and band 3 were in an extended configuration.

In conclusion, single photon radioluminescence is a powerful biophysical technique to address questions about submicroscopic distances and molecular transport that cannot be examined readily by other techniques. Notwithstanding the relatively large amounts of radioactivity required currently and the small single photon signal intensities, the radioluminescence method should have a wide range of applications in biochemistry, and membrane and cell biology.

We thank Drs. Uri Galili and Dr. Richard Anderson for advice on the lectin binding studies, Dr. Bernard Thevenin for advice and discussions, Dan Smuckler for assistance in the construction of the rapid injection device, and Daniel Zimmet for invaluable technical and computer assistance.

Funds for the gated photon counter were provided by a grant from the UCSF Academic Senate. This work was supported by grants DK16095 and DK43840 from the National Institutes of Health. Dr. Verkman is an established investigator of the American Heart Association. This is publication number 122 of the MacMillan-Cargill Hematology Laboratory.

Received for publication 2 March 1992 and in final form 20 July 1992.

REFERENCES

Adair, W., and S. Kornfeld. 1974. Isolation of receptors for wheat germ agglutinin and the Ricinus communis lectins from human erythrocytes using affinity chromatography. *J. Biol. Chem.* 249:4696–4704.

Bicknese, S., and M. F. Maestre. 1987. Correction of fluorescence detected circular dichroic photoselection artifacts using light collecting ellipsoidal mirrors. *Rev. Sci. Instrum.* 58:2060–2063.

Bicknese, S., Z. Shahrokh, S. B. Shohet, and A. S. Verkman. 1992. Single photon radioluminescence. I. Theory and spectroscopic properties. *Biophys. J.* 63:1256–1266.

Bjerrum, P. J. 1979. Hemoglobin-depleted human erythrocyte ghosts: characterization of morphology and transport functions. *J. Membr. Biol.* 48:43–67.

Bradford, M. M. 1976. A rapid sensitive method for the quantitation of microgram quantities of protein utilizing the principle of protein-dye binding. *Anal. Biochem.* 72:248.

Broring, K., C. W. M. Haest, and B. Deuticke. 1989. Translocation of oleic acid across the erythrocyte membrane. Evidence for a fast process. *Biochim. Biophys. Acta.* 986:321–331.

Brown, J. R., and P. Sckockley. 1982. Serum albumin:structure and characterization of its ligand binding sites. *In* Lipid-protein interactions. P. C. Jost and O. H. Griffith, editors. John Wiley & Sons, New York. 26–68.

Cabantchik, Z. I., and A. Rothstein. 1974. Membrane proteins related to anion permeability of human red blood cells. *J. Membr. Biol.* 15:207–226.

Cistola, D. P., D. M. Small, and J. A. Hamilton. 1987. Carbon 13 NMR studies of saturated fatty acids bound to bovine serum albumin. I. the filling of individual fatty acid binding sites. *J. Biol. Chem.* 262:10971–10979.

Danilov, Y. N., and C. M. Cohen. 1989. Wheat germ agglutinin but not concanavalin A modulates protein kinase C-mediated phosphorylation of red cell skeletal proteins. *FEBS Lett.* 257:431–434.

Dive, C., C. Hilary, J. V. Watson, and P. Workman. 1988. Polar fluorescein derivatives as improved substrate probes for flow cytoenzymological assay of cellular esterases. *Mol. Cell. Probes.* 2:131–145.

Dodge, J. T., C. Mitchell, and D. J. Hanahan. 1963. The preparation and chemical characteristics of hemoglobin-free ghosts of human erythrocytes. *Arch. Biochem. Biophys.* 100:119–130.

Halbhuber, K. J., H. Oehring, M. Gliesing, and D. Stibenz. 1990. Polarization-optical investigation (topo-optical analysis) of the structure of the human erythrocyte glycocalyx. Influence of pH, ionic strength, and diamide-induced spectrin crosslinking. *Cell. Mol. Biol.* 36:643–657.

Hirayama, K., S. Akashi, M. Furuya, and K. Fukuhara. 1990. Rapid confirmation and revision of the primary structure of bovine serum albumin by ESIMS and FRIT-FAB LC/MS. *Biochem. Biophys. Res. Commun.* 173:639–646.

Hirayama, F., and S. Lipsky. 1971. Saturated hydrocarbons as donors in electronic energy transfer processes. *In* Organic scintillators and liquid scintillation counting. D. L. Horrocks and C.-T. Peng, editors. Academic Press, New York. 205–221.

Huang, C. 1969. Studies on phosphatidylcholine vesicles. Formation and physical characteristics. *Biochemistry.* 8:344–351.

Ivatt, R. J., P. B. Harnett, and J. W. Reeder. 1986. Isolated erythrocglycans have a high-affinity interaction with wheat germ agglutinin but are poorly accessible in situ. *Biochim. Biophys. Acta.* 881:124–134.

Jung, C. Y., L. M. Carlson, and D. A. Whaley. 1971. Glucose transport carrier activities in extensively washed human red cell ghosts. *Biochim. Biophys. Acta.* 241:613–627.

Jung, C. Y., and A. L. Rampal. 1977. Cytochalasin B binding sites and glucose transport carrier in human erythrocyte ghosts. *J. Biol. Chem.* 252:5456–5463.

Kragh-Hansen, U. 1989. Structure and ligand binding properties of human serum albumin. *Danish Med. Bull.* 37:57–84.

Lepke, S., H. Fasold, M. Pring, and H. Passow. 1976. A study of the relationship between inhibition of anion exchange and binding to the red blood cell membrane of 4,4′-diisothiocyano stilbene-2,2′-disulfonic acid (DIDS) and its dihydro derivative (H_2DIDS). *J. Membr. Biol.* 29:147–177.

Lovrien, R. E., and R. A. Anderson. 1980. Stoichiometry of wheat germ agglutinin as a morphology controlling agent and as a morphology protective agent for the human erythrocyte. *J. Cell Biol.* 85:534–548.

Lund-Katz, S., H. M. Laboda, L. R. McLean, and M. C. Phillips. 1988.

Influence of molecular packing and phospholipid type on rates of cholesterol exchange. *J. Biol. Chem.* 27:3416–3423.

Scott, T. G., R. D. Spencer, N. J. Leonard, and G. Weber. 1970. Emission properties of NADH. Studies of fluorescence lifetimes and quantum efficiencies of NADH, AcPyADH, and simplified synthetic models. *J. Am. Chem. Soc.* 92:687–695.

Spector, A. A., and K. M. John. 1968. Effects of free fatty acid on the fluorescence of bovine serum albumin. *Arch. Biochem. Biophys.* 127:65–71.

Storch, J., and A. M. Kleinfeld. 1986. Transfer of long-chain fluorescent free fatty acids between unilamellar vesicles. *Biochemistry.* 25:1717–1726.

Stryer, L. 1978. Fluorescence energy transfer as a spectroscopic ruler. *Annu. Rev. Biochem.* 47:819–846.

Tanner, M. J. A., P. G. Martin, and S. High. 1988. The complete amino acid sequence of the human erythrocyte membrane anion-transport protein deduced from the cDNA sequence. *Biochem. J.* 256:703–712.

Thulborn, K. R., and W. H. Sawyer. 1978. Properties and the locations of a set of fluorescent probes sensitive to the fluidity gradient of the lipid bilayer. *Biochim. Biophys. Acta.* 511:125–140.

Viitala, J., and J. Jarnefelt. 1985. The red cell surface revisited. *TIBS.* 10:392–395.

Von Tscharner, V., and G. K. Radda. 1980. A study of changes in surface area and molecular interactions in phospholipid vesicles by condensed phase radioluminescence. *Biochim. Biophys. Acta.* 601:63–77.

Von Tscharner, V., and G. K. Radda. 1981. The effect of fatty acids on the surface potential of phospholipid vesicles measured by condensed phase radioluminescence. *Biochim. Biophys. Acta.* 643:435–448.

Weber, G., and F. W. J. Teale. 1957. Determination of the absolute quantum yield of fluorescent solutions. *Trans. Farad. Soc.* 23:646–655.

Wheeler, J., and P. C. Hinkle. 1985. The glucose transporter of mammalian cells. *Annu. Rev. Physiol.* 47:503–517.

Weisiger, R. A., and W. L. Ma. 1987. Uptake of oleate from albumin solutions by rat liver. *J. Clin. Invest.* 79:1070–1077.